ORTHOGONAL PRECODING FOR SIDELOBE SUPPRESSION IN DFT-BASED SYSTEMS USING BLOCK REFLECTORS

I. Vaughan L. Clarkson

P.O. Box 920, Samford Village, Qld., 4520, AUSTRALIA, v.clarkson@ieee.org.

ABSTRACT

Sidelobe suppression has always been an important part of crafting communications signals to keep interference with users of adjacent spectrum to a minimum. Systems based on the discrete Fourier transform, such as orthogonal frequency-division multiplexing (OFDM) and single-carrier frequency-division multiple access (SC-FDMA) are especially prone to out-of-band power leakage. Although many techniques have been proposed to suppress sidelobes in DFT-based systems, a satisfactory balance between computational complexity and out-of-band power leakage has remained elusive.

Orthogonal precoding is a promising, linear technique in which the nullspace of a precoding matrix with orthonormal columns is designed to suppress the sidelobes. In particular, Xu and Chen [1], van de Beek [2] and Ma *et al.* [3] have proposed orthogonal precoders that yield excellent out-of-band suppression. However, they suffer from high arithmetic complexity—quadratic in the number of active subcarriers—which has limited their application.

In this paper, we find that the arithmetic complexity can be made linear instead of quadratic if a *block reflector* is used to perform the precoding instead of an otherwise unstructured unitary transformation. There is no penalty to be paid in achieved bit-error rate. We show by numerical simulation that the penalty in peak-to-average power ratio is also very small for OFDM.

Index Terms— OFDM, SC-FDMA, orthogonal precoding, sidelobe suppression, block reflector.

1. INTRODUCTION

With the ready availability of advanced digital signal processing in modern communications systems, the advantages conferred by the discrete Fourier transform (DFT) are routinely exploited. The DFT lies at the heart of orthogonal frequency division multiplexing and OFDM is now common to many major global communications standards for digital subscriber lines, cable broadband, wireless local area networks, digital video and audio broadcasting and fourth-generation mobile broadband. Use of the DFT in OFDM improves spectral density, simplifies channel equalisation and minimises inter-symbol interference (ISI) from multi-path propagation. In an OFDM transmitter, portions of its bandwidth can be turned on and off flexibly under software control. This is the principle that underpins orthogonal frequency-division multiple access (OFDMA). It also makes OFDM an attractive candidate for cognitive radio [4].

OFDM is not without its disadvantages. For instance, it is sensitive to Doppler diversity. However, the two disadvantages that will concern us in this paper are its high out-of-band spectral leakage and peak-to-average power ratio (PAPR).

Standard OFDM exhibits sidelobes which, away from the central band, diminish in power spectral density in proportion to the inverse square of the frequency. Relatively wide guard bands are needed to keep the amount of interference with adjacent users to acceptable limits. In cognitive radio, where narrow unused gaps in the spectrum are to be exploited, wide guard bands are especially deleterious.

In 5th-generation (5G) mobile wireless, supporting the "Internet of Things" will require device-to-device (D2D) communication on a much greater scale than is seen presently [5, 6]. The emerging paradigm is sometimes called "Massive Machine-Type Communication". D2D communication is typically low-rate and low-power. To accommodate D2D, 5G standards may relax synchronisation requirements in order to allow communicating devices to conserve power [7–9]. So, like cognitive radio, D2D communication in 5G would need to exploit narrow "slots" in the available spectrum while only coarsely synchronised with other transmitters. Wide guard bands again cannot be tolerated.

For these reasons, there have been many proposals for schemes to reduce out-of-band radiation in OFDM. OFDM symbols can be filtered in the time domain to achieve arbitrarily high attenuation of sidelobes, but this introduces ISI [10]. OFDM symbols may be windowed or undergo pulse-shaping, cyclic prefixes may be extended or subcarriers at the edge of the band may be deactivated, but this reduces spectral efficiency [10–12]. These may all be termed linear approaches to sidelobe suppression.

Non-linear approaches have been studied too. Adaptive symbol transition [13] optimises short, non-information-bearing signal segments to be inserted between adjacent symbols to suppress sidelobes but again this reduces spectral efficiency. Cancellation carriers [14] are sub-carriers that are reserved to actively cancel sidelobe power. Spectral efficiency is reduced while PAPR is increased. Subcarrier weighting [15] involves computing an optimal weighting on each subcarrier to suppress out-of-band power but may degrade bit-error rate (BER). The multiple-choice sequence method [16] involves generating several candidate symbols using a set of agreed rules and selecting the one for transmission that best suppresses out-of-band power. However, like the selected mapping technique [17] for PAPR reduction from which it is derived, it requires side information.

Linear precoding is the method that will occupy our attention. Here, the data for transmission undergoes a linear transformation designed to confer some benefit. Different precoding schemes have been proposed for OFDM to counteract channel effects, suppress ICI, and reduce PAPR—see [18] and references therein—but the approach can also be applied to sidelobe suppression. Some of the proposals introduce correlation that degrade the orthogonality within each OFDM symbol [19–22]. BER increases as a consequence. In contrast, orthogonal precoding, as first proposed by Chung [18], does not increase the BER. Yet there is some loss of spectral efficiency because degrees of freedom are sacrificed in the OFDM symbol. There is also a notable increase in computational complexity.

Orthogonal linear precoding, as independently proposed by Xu and Chen [1], van de Beek [2] and Ma *et al.* [3], uses the null space of a precoding matrix with orthonormal columns to shape the spectrum of the transmitted symbol. The dimension of the null space is kept as small as possible in order to conserve the degrees of freedom available for data transmission. The precoding matrix is therefore approximately square. With the precoding matrix regarded as an otherwise unstructured matrix, multiplication of the precoding matrix with the data vector is a relatively expensive operation. Its arithmetic complexity is quadratic in the number of active subcarriers.

In this paper, we make the straightforward observation that the precoding matrix for orthogonal precoding need not be unstructured. We propose instead to use a block reflector [23, 24]. A block reflector is a generalisation of the Householder transformation. A Householder transformation is a unitary transform—a reflection—that maps a specified one-dimensional subspace to another. The arithmetic complexity of a Householder transformation is linear, rather than quadratic, in the dimension of the vector it transforms. Block reflectors generalise this notion to map between subspaces of arbitrary dimension. If the dimension of the subspace is regarded as constant, the arithmetic complexity of block reflection is likewise linear in the dimension of the vector undergoing reflection. Thus, block reflection dramatically reduces the computational cost of orthogonal precoding.

Compared to standard orthogonal precoding, using a block reflector does not alter the BER properties, since the precoding remains orthogonal, nor does it alter the spectral properties. In numerical simulations based on the E-UTRA standard for 4G mobile communications [25], we show that the effect on PAPR is almost negligible for OFDM, such as is used for downlink in E-UTRA, at less than $0.1\,\mathrm{dB}$. When adapted for single-carrier frequency-division multiple access (SC-FDMA), as used for uplink in E-UTRA, we demonstrate that block reflector precoding is not discernibly worse than the orthogonal precoder of Ma *et al.* [3], which aims to minimise PAPR.

2. SYSTEM MODEL

We make use of a standard model to represent a DFT-based communications system which is general enough to encompass both OFDM and SC-FDMA. A block diagram is presented in Figure 1.

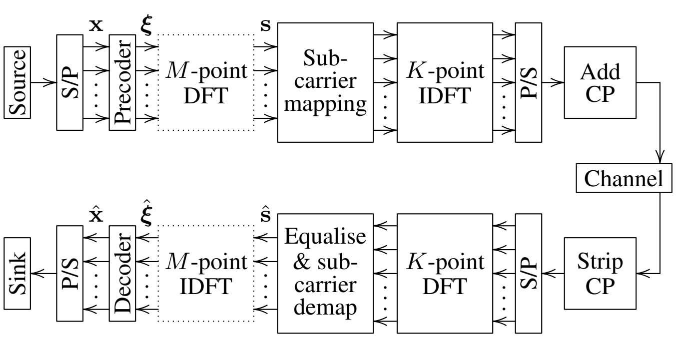

Fig. 1. DFT-based communications system.

At the transmitter, complex-valued symbols emanate from the source with the data encoded in the symbols using a modulation format such as QPSK or QAM. The symbols are then aggregated into groups of length N to form the OFDM symbol as they pass through the serial-to-parallel converter (S/P). Such a group of symbols can be represented in an *uncoded symbol vector*, $\overline{\mathbf{x}} \in \mathbb{C}^N$. A precoding matrix $\overline{\mathbf{P}} \in \mathbb{C}^{M\times N}$, $M > N$, with orthonormal columns, $\overline{\mathbf{P}}^H\overline{\mathbf{P}} = \mathbf{I}$, is used to generate a new vector $\boldsymbol{\xi}$, the *precoded symbol vector*. In SC-FDMA, the vector is additionally Fourier-transformed. The resulting *subcarrier mapping input vector*, $\mathbf{s}$, contains the complex amplitudes which will be assigned to the subcarriers. That is, $\mathbf{s} = \boldsymbol{\xi} = \overline{\mathbf{P}}\overline{\mathbf{x}}$ or $\mathbf{s} = \mathbf{W}\boldsymbol{\xi} = \mathbf{W}\overline{\mathbf{P}}\overline{\mathbf{x}}$ for OFDM or SC-FDMA, respectively, where $\mathbf{W}$ is the matrix of coefficients of the unitary DFT. To unify the notation, we can write $\mathbf{s} = \overline{\mathbf{Q}}\overline{\mathbf{x}}$ where $\overline{\mathbf{Q}} = \overline{\mathbf{P}}$ for OFDM or $\overline{\mathbf{Q}} = \mathbf{W}\overline{\mathbf{P}}$ for SC-FDMA.

Since the uncoded symbol vector $\overline{\mathbf{x}}$ has smaller dimension than the precoded symbol vector, we observe that there is a coding rate $\lambda = N/M$ which is less than unity. We will find it convenient on occasion to consider an uncoded symbol vector that has the same dimension as the precoded vector. Define the *zero-padded* uncoded symbol vector $\mathbf{x}$ as

$$\mathbf{x} = \begin{pmatrix} \mathbf{0}_R \\ \overline{\mathbf{x}} \end{pmatrix}$$

where $\mathbf{0}_R$ is a vector of all zeros having dimension $R = M - N$. Correspondingly, $\mathbf{s} = \boldsymbol{\xi} = \mathbf{P}\mathbf{x}$ or $\mathbf{s} = \mathbf{W}\boldsymbol{\xi} = \mathbf{W}\mathbf{P}\mathbf{x}$ for OFDM or SC-FDMA, respectively, where $\mathbf{P}$ is formed by prepending orthonormal column vectors to $\overline{\mathbf{P}}$ to complete a basis of $\mathbb{C}^M$. That is, $\mathbf{P}$ is a unitary matrix. As before, to unify the notation, we can simply write $\mathbf{s} = \mathbf{Q}\mathbf{x}$.

The subcarrier amplitudes $s_1, \ldots, s_M$ are mapped to subcarriers $k_1, \ldots, k_M$ where each k_i lies within an interval of length $K \geqslant M$. A K-point inverse DFT produces a discrete-time signal segment in vector form. The parallel-to-serial converter (P/S) reads the samples out of the vector serially and a cyclic prefix (CP) is prepended.[1] The OFDM or SC-FDMA symbol so assembled is then converted to analog, filtered, amplified, up-converted and radiated where it passes through the channel to the receiver.

At the receiver, these operations are undone in reverse order, with $\hat{\mathbf{s}}$, $\hat{\boldsymbol{\xi}}$ and $\hat{\mathbf{x}}$ being the received approximations of $\mathbf{s}$, $\boldsymbol{\xi}$ and $\mathbf{x}$.

The complex baseband continuous-time signal segment output by the digital-to-analog converters in the transmitter has the form $y(t) = \sum_{i=1}^{M} s_i \exp(j2\pi k_i f_\mathrm{s} t)$ for $-T_\mathrm{cp} \leqslant t < T_\mathrm{s}$ where f_s is the subcarrier spacing, $T_\mathrm{s} = 1/f_\mathrm{s}$ is the useful symbol duration and T_cp is the CP duration. The sum $T = T_\mathrm{cp} + T_\mathrm{s}$ is the symbol period.

With $y(t)$ assumed to be zero outside the time interval $[-T_\mathrm{cp}, T_\mathrm{s})$, its spectrum is $Y(f) = \sum_{i=1}^{M} a_i^*(f) s_i$ where

$$a_i(f) = T \exp\left[-j\pi(T_\mathrm{s} - T_\mathrm{cp})(f - k_i f_\mathrm{s})\right] \cdot \operatorname{sinc}\left[\pi(T_\mathrm{s} + T_\mathrm{cp})(f - k_i f_\mathrm{s})\right]$$

and $\operatorname{sinc}(x) \triangleq \sin(x)/x$. With the functions $a_i(f)$, $i = 1, \ldots, M$, grouped as a column vector $\mathbf{a}(f)$, we have $Y(f) = \mathbf{a}^H(f)\mathbf{s}$.

Given that the transmitted signal is a train of symbols of the form $y(t)$ transmitted serially, end-to-end, and with each symbol assumed to be independent of all others, the power spectral density is [3, 21]

$$G_Y(f) = \frac{\eta}{T} \|\overline{\mathbf{Q}}^H \mathbf{a}(f)\|^2 \tag{1}$$

where η is the power assigned to each symbol in the source stream, *i.e.*, the power assigned to each element of $\overline{\mathbf{x}}$.

3. SIDELOBE SUPPRESSION

To suppress sidelobes, van de Beek [2] proposes selecting a set of out-of-band frequencies $\mathcal{M} = \{f_1, \ldots, f_R\}$ such that the PSD

[1] Although CP is specified in this system model, orthogonal precoding is also applicable and effective when zero padding (ZP) is used instead of CP.

$G_Y(f_r) = 0$ for $r = 1, \ldots, R$. It follows from (1) that the vectors $\mathbf{a}(f_1), \ldots, \mathbf{a}(f_R)$ should be in the nullspace of $\overline{\mathbf{Q}}^H$. That is, if we construct a matrix $\mathbf{C}_{\text{vdB}} = (\mathbf{a}(f_1), \ldots, \mathbf{a}(f_R))$ then $\overline{\mathbf{Q}}^H \mathbf{C}_{\text{vdB}} = \mathbf{0}$. As van de Beek states, while "there are no guarantees that the emitted power at frequencies other than those in $\mathcal{M}$ is small, results in [21] indicate that they are for a number of well-chosen sets $\mathcal{M}$."

On the other hand, Ma *et al.* [3] propose that, at a discrete set of out-of-band frequencies ϕ, we design $\overline{\mathbf{Q}}$ to minimise $\sum_{f \in \phi} G_Y(f)$. That is, we construct the matrix $\mathbf{C}_{\text{Ma}}$ whose columns are $\mathbf{a}(f)$ for each $f \in \phi$ and set $\overline{\mathbf{Q}}$ as the minimiser of $\|\overline{\mathbf{Q}}^H \mathbf{C}_{\text{Ma}}\|_{\text{F}}^2$, where $\|\cdot\|_{\text{F}}$ is the Frobenius norm.

The approach of Xu and Chen [1] is similar to, but precedes, that of Ma *et al.* Their proposal is couched in the language of spectrum pooling and seeks to maximise what they call the "contrast energy ratio" for a secondary user within unused licensed spectrum. It results in a generalised Hermitian eigenvalue problem from which the eigenvectors of the N smallest eigenvalues are gathered to form $\overline{\mathbf{Q}}$.

In the approaches of both van de Beek and Ma *et al.*, we find $\overline{\mathbf{Q}}$ by first finding $\mathbf{Q}$ from a singular value decomposition (SVD) of the $\mathbf{C}$ matrix, either $\mathbf{C}_{\text{vdB}}$ or $\mathbf{C}_{\text{Ma}}$. We write the SVD as

$$\mathbf{C} = \mathbf{U}\boldsymbol{\Sigma}\mathbf{V}^H \tag{2}$$

where $\mathbf{U}$ and $\mathbf{V}$ are unitary and $\boldsymbol{\Sigma}$ is diagonal with non-negative real elements (the singular values) on the diagonal in descending order. It can be shown that $\mathbf{Q} = \mathbf{U}$ is a suitable choice to achieve sidelobe suppression [2, 3]. We partition $\mathbf{U}$ so that $\mathbf{U} = (\tilde{\mathbf{U}}, \overline{\mathbf{U}})$ where $\tilde{\mathbf{U}}$ represents the first R columns of $\mathbf{U}$ and $\overline{\mathbf{U}}$ the remaining N columns. It is then clear that $\overline{\mathbf{Q}} = \overline{\mathbf{U}}$.

Although $\mathbf{Q} = \mathbf{U}$ is a suitable choice to achieve sidelobe suppression in either of the two approaches, it isn't the only choice for $\mathbf{Q}$. Any choice for $\mathbf{Q}$ of the form $\mathbf{Q} = (\tilde{\mathbf{U}}\tilde{\boldsymbol{\Psi}}, \overline{\mathbf{U}\boldsymbol{\Psi}})$ is also admissible for any unitary matrices $\tilde{\boldsymbol{\Psi}}$ and $\overline{\boldsymbol{\Psi}}$. Ma *et al.* [3] go on to propose a method to select a particular value for $\overline{\boldsymbol{\Psi}}$ that reduces PAPR. Our aim is to derive an admissible $\mathbf{Q}$ that allows fast computation of $\mathbf{Qx}$.

4. BLOCK REFLECTORS

A *Householder reflection* is a computationally efficient method that is widely used in numerical linear algebra to effect a unitary transformation mapping vectors from a specified one-dimensional subspace to another (and vice versa) [26, 27]. If $\mathbf{y} \neq \mathbf{z}$ are unit basis vectors for the two subspaces then the *Householder matrix*

$$\mathbf{H} = \mathbf{I} - \mathbf{g}\mathbf{g}^H \qquad \text{where} \qquad \mathbf{g} = \sqrt{2}\frac{\mathbf{y} - \mathbf{z}}{\|\mathbf{y} - \mathbf{z}\|} \tag{3}$$

does what is required, namely, as can be readily verified, it is unitary, $\mathbf{Hy} = \mathbf{z}$ and $\mathbf{Hz} = \mathbf{y}$. Because the basis vectors are not unique, it follows that the Householder matrix to effect the desired reflection is also not unique.

At first glance, it would appear that the arithmetic complexity—the number of floating-point operations—necessary to compute a Householder reflection on a vector $\mathbf{v}$ is proportional to the square of the dimension of $\mathbf{v}$, since computation of $\mathbf{Hv}$ is an instance of matrix-vector multiplication. However, observing that $\mathbf{Hv} = \mathbf{v} - \mathbf{g}(\mathbf{g}^H\mathbf{v})$, we can see that the Householder reflection can instead be computed using an inner product, a scalar-vector multiplication and a vector subtraction. The complexity of each of these operations is only linear in the dimension of $\mathbf{v}$.

A *generalised Householder reflection* is a unitary transformation that maps between a pair of specified subspaces with dimension $\rho > 1$. Suppose $\mathbf{Y}$ is a matrix whose ρ columns form an orthonormal basis of one subspace and $\mathbf{Z}$ likewise yields the basis of the other. Further suppose that the singular value decomposition of $\mathbf{Y}^H\mathbf{Z}$ is $\boldsymbol{\Theta}\mathbf{D}\boldsymbol{\Phi}^H$ and that all the singular values are less than unity (*i.e.,* the intersection of the two subspaces contains only $\mathbf{0}$). A *block reflector* $\mathbf{H}$ can be derived in the form

$$\mathbf{H} = \mathbf{I} - \mathbf{G}\mathbf{G}^H \qquad \text{where} \qquad \mathbf{G} = (\mathbf{Y}\boldsymbol{\Theta} - \mathbf{Z}\boldsymbol{\Phi})(\mathbf{I} - \mathbf{D})^{-1/2} \tag{4}$$

We can verify that $\mathbf{H}$ is unitary, $\mathbf{HY}\boldsymbol{\Theta} = \mathbf{Z}\boldsymbol{\Phi}$ and $\mathbf{HZ}\boldsymbol{\Phi} = \mathbf{Y}\boldsymbol{\Theta}$.

For fixed ρ, the arithmetic complexity of computing a generalised Householder reflection on a vector $\mathbf{v}$ using a block reflector is linear, rather than quadratic, in the dimension of $\mathbf{v}$. Numerically stable algorithms for calculating block reflectors based on the polar and Cholesky decompositions have been derived [23, 24]. Like Householder matrices, block reflectors are not unique for any specified pair of subspaces.

5. BLOCK REFLECTORS FOR SIDELOBE SUPPRESSION

To achieve sidelobe suppression using block reflectors, we construct a block reflector that maps from the subspace spanned by $\mathbf{e}_1, \ldots, \mathbf{e}_R$, where $\mathbf{e}_i$ is the i^{th} column of the identity matrix, to the subspace spanned by the first R columns of $\mathbf{U}$ in (2) for OFDM or of $\mathbf{W}^H\mathbf{U}$ for SC-FDMA, *i.e.*, $\tilde{\mathbf{U}}$ or $\mathbf{W}^H\tilde{\mathbf{U}}$, respectively. The resulting block reflector, $\mathbf{H}$, has the properties we require for sidelobe suppression. That is, the first R columns of $\mathbf{H}$ span the same subspace as $\tilde{\mathbf{U}}$ (respectively, $\mathbf{W}^H\tilde{\mathbf{U}}$) and the remaining columns span a subspace which is orthogonal to it. It follows that $\mathbf{H}$ is an acceptable assignment for $\mathbf{P}$, the precoding matrix. From (4), a computationally efficient way to compute the precoded symbol vector $\boldsymbol{\xi}$ is to evaluate the expression $\boldsymbol{\xi} = \mathbf{x} - \mathbf{G}(\mathbf{G}^H\mathbf{x})$. In doing so, the computational cost of performing orthogonal precoding becomes linear rather than quadratic in N, if we take R to be a constant. Formally, the computational cost is $O(MR)$.

Being a reflector, $\mathbf{H}$ has the property that $\mathbf{H}^2 = \mathbf{I}$. Therefore, at the receiver, the orthogonal decoding operation can be written $\hat{\mathbf{x}} = \hat{\boldsymbol{\xi}} - \mathbf{G}(\mathbf{G}^H\hat{\boldsymbol{\xi}})$. We see that computational cost is again linear in N.

This overcomes what is viewed as a major impediment to orthogonal precoding (and decoding). For instance, in proposing a resource-block precoded OFDM scheme in [28], Fang *et al.* motivate their investigation in part by noting that "the complexity [of orthogonal precoding and decoding] has order of $O(N^2)$, which is unacceptable when N is large." In the same vein, Zheng *et al.* [29], introducing their own low-complexity precoding technique based on [20], observe that "conventional [orthogonal precoding needs] computations between matrices with great dimensions and are always too complicated especially when the number of available subcarriers is large." As a last example, Zhang *et al.* [22] motivate their projection precoding proposal by remarking that "both approaches [1, 3] have the advantage of maintaining the receiver SNR, but their computation complexity is proportional to the square of the number of subcarriers."

6. SIMULATION RESULTS

Results are presented here to demonstrate the power of orthogonal precoding using block reflectors to suppress sidelobes and to explore its effect on PAPR in OFDM and SC-FDMA. No results are presented for BER as the BER properties are unchanged with respect to orthogonal precoders as they were originally described in [1–3].

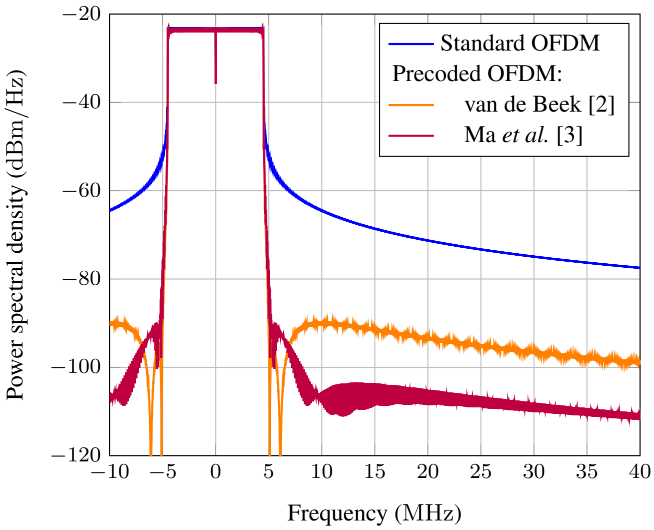

Fig. 2. Power spectral density of orthogonally precoded OFDM signals based on E-UTRA parameters [25].

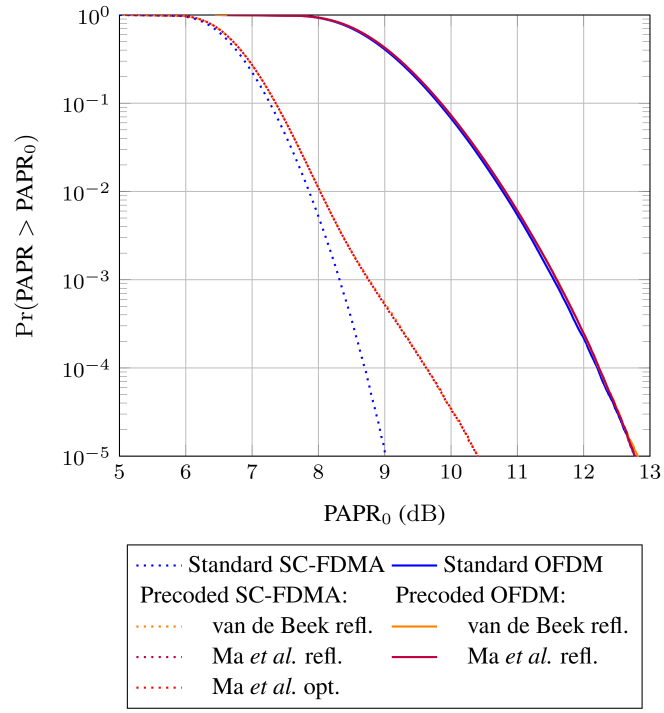

Fig. 3. CCDF of PAPR of orthogonal precoding schemes based on E-UTRA parameters [25].

In Figure 2, a scenario used by van de Beek [2] is recreated to demonstrate the effectiveness of orthogonal precoding to suppress sidelobes. It is inspired by (4G) E-UTRA/LTE parameters [25]. Of $K = 2048$ available subcarriers at $15\,\text{kHz}$ spacing, $M = 600$ subcarriers are modulated using QPSK with a subcarrier mapping such that $-300 \leqslant k_i \leqslant 300$, $k_i \neq 0$. For the cyclic prefix, $T_{\text{cp}} = 9T_{\text{s}}/128$. The transmitted power is $46\,\text{dBm}$. Standard OFDM exhibits the characteristic "flat top" to its power spectral density of approximately $-23\,\text{dBm/Hz}$. There is a slow decay of the power in the sidelobes, not quite reaching $-80\,\text{dBm/Hz}$ at a distance of $40\,\text{MHz}$ from the centre frequency. SC-FDMA spectral properties with the same parameters are identical to those shown for OFDM.

The PSDs resulting from the orthogonal precoding methods of van de Beek [2] and Ma *et al.* [3] are also plotted in Figure 2. In both cases, we use block reflectors. We set $R = 8$, so $N = 592$ and the coding rate falls slightly to $592/600$. For the van de Beek approach, the spectrum is nulled at the frequencies $\pm 5100 \pm 1$ and $\pm 6100 \pm 1\,\text{kHz}$. The out-of-band PSD is dramatically lower than standard OFDM, almost universally $20\,\text{dBm/Hz}$ lower. For the Ma *et al.* approach, spectral leakage is minimised at frequencies from $-40\,\text{MHz}$ to $-5\,\text{MHz}$ and from $5\,\text{MHz}$ to $40\,\text{MHz}$, sampled at intervals of $200\,\text{kHz}$. A further out-of-band attenuation of approximately $10\,\text{dBm/Hz}$ is evident.

In Figure 3, the complementary cumulative distribution function (CCDF) of PAPR is examined for orthogonal precoding using block reflectors. The parameters of the OFDM scenario are carried over from Figure 2. The method for calculating PAPR is taken from [3] with ten million independent trials to generate the CCDF for each method. We see that the solid lines representing OFDM PAPR all but coincide. The PAPR penalty for orthogonal precoding is $\ll 0.1\,\text{dB}$.

A slightly more diverse picture presents itself for SC-FDMA. It is clear that each of the orthogonal precoding techniques for SC-FDMA incurs a penalty with respect to standard SC-FDMA. The penalty appears to be identical regardless of the precoding method. That is, the PAPR CCDFs for the block-reflector-based methods (marked "refl." in the legend) appear to coincide with each other and with the PAPR-optimised method of [3, §IIIC] (marked "opt." in the legend) that does not use block reflectors.

Down to a probability of 10^{-3}, the PAPR penalty of orthogonal precoding does not exceed $0.5\,\text{dB}$ but, below that point, the penalty noticeably increases to nearly $1.5\,\text{dB}$ at a probability of 10^{-5}. There is always an advantage of at least $2\,\text{dB}$ compared with OFDM.

7. CONCLUDING REMARKS

Orthogonal precoding is a linear technique for suppressing out-of-band energy in DFT-based communication systems such as OFDM and SC-FDMA. Its frequently cited drawback is that its arithmetic complexity increases according to the square of the number of active subcarriers, which is considered unacceptably high. In this paper, we have shown that, by using block reflectors, the arithmetic complexity can instead be made linear in the number of subcarriers.

Through a simulation scenario inspired by E-UTRA/LTE, we have demonstrated that orthogonal precoding using block reflectors achieves excellent sidelobe suppression. For OFDM, there is almost no PAPR penalty to be seen for using orthogonal precoding—less than $0.1\,\text{dB}$. For SC-FDMA, a penalty is evident, not exceeding $1.5\,\text{dB}$, but the penalty is no greater for the use of block reflectors as against other orthogonal precoders.

As a final remark, we observe that block reflectors are not the only means by which the arithmetic complexity can be made linear in the number of subcarriers. Block reflectors have been preferred here for their appealing simplicity in presentation. The WY representation for products of Householder reflections could have been substituted with little difficulty [27, 30, 31], as could a basis-kernel representation [32]. Indeed, products of Householder reflections could have been substituted directly.

8. REFERENCES

[1] R. Xu and M. Chen, "A precoding scheme for DFT-based OFDM to suppress sidelobes," *IEEE Commun. Letters*, vol. 13, no. 10, pp. 776–778, Oct. 2009.

[2] J. van de Beek, "Orthogonal multiplexing in a subspace of frequency well-localized signals," *IEEE Commun. Letters*, vol. 14, no. 10, pp. 882–884, Oct. 2010.

[3] M. Ma, X. Huang, B. Jiao, and Y. J. Guo, "Optimal orthogonal precoding for power leakage suppression in DFT-based systems," *IEEE Trans. Commun.*, vol. 59, no. 3, pp. 844–853, Mar. 2011.

[4] T. A. Weiss and F. K. Jondal, "Spectrum pooling: An innovative strategy for the enhancement of spectrum efficiency," *IEEE Commun. Mag.*, pp. S8–S14, Mar. 2004, Radio Communications Supplement.

[5] G. Wunder, M. Kasparick, S. ten Brink, F. Schaich, T. Wild, I. Gaspar, E. Ohlmer, S. Krone, N. Michailow, A. Navarro, G. Fettweis, D. Ktenas, V. Berg, M. Dryjanski, S. Pietrzyk, and B. Eged, "5GNOW: Challenging the LTE design paradigms of orthogonality and synchronicity," in *Proc. IEEE Vehic. Technol. Conf. Spring*, Jun. 2013.

[6] A. Osseiran, F. Boccardi, V. Braun, K. Kusume, P. Marsch, M. Maternia, O. Queseth, M. Schellmann, H. Schotten, H. Taoka, H. Tullberg, M. A. Uusitalo, B. Timus, and M. Fallgren, "Scenarios for 5G mobile and wireless communications: The vision of the METIS project," *IEEE Commun. Mag.*, vol. 52, no. 5, pp. 26–35, May 2014.

[7] T. Wild, F. Schaich, and Y. Chen, "5G air interface design based on universal filtered (UF-)OFDM," in *Proc. Internat. Conf. Digital Signal Process.*, Aug. 2014, pp. 699–704.

[8] J.-B. Doré, V. Berg, and D. Ktenas, "Performance of FBMC multiple access for relaxed synchronization cellular networks," in *Proc. Internat. Conf. Global Telecomm.*, Dec. 2014, pp. 983–988.

[9] J. Abdoli, M. Jia, and J. Ma, "Filtered OFDM: A new waveform for future wireless systems," in *Proc. Signal Process. Advances Wireless Commun.*, Jun. 2015, pp. 66–70.

[10] M. Faulkner, "The effect of filtering on the performance of OFDM systems," *IEEE Trans. Vehic. Technol.*, vol. 49, no. 5, pp. 1877–1884, Sep. 2000.

[11] A. Vahlin and N. Holte, "Optimal finite duration pulses for OFDM," *IEEE Trans. Commun.*, vol. 44, no. 1, pp. 10–14, Jan. 1996.

[12] T. Weiss, J. Hillenbrand, A. Krohn, and F. K. Jondal, "Mutual interference in OFDM-based spectral pooling systems," in *Proc. IEEE Vehic. Technol. Conf. Spring*, vol. 4, May 2004, pp. 1873–1877.

[13] H. A. Mahmoud and H. Arslan, "Sidelobe suppression in OFDM-based spectrum sharing using adapting symbol transition," *IEEE Commun. Letters*, vol. 12, no. 2, pp. 133–135, Feb. 2008.

[14] S. Brandes, I. Cosovic, and M. Schnell, "Reduction of out-of-band radiation in OFDM systems by insertion of cancellation carriers," *IEEE Commun. Letters*, vol. 10, no. 6, pp. 420–422, Jun. 2006.

[15] I. Cosovic, S. Brandes, and M. Schnell, "Subcarrier weighting: A method for sidelobe suppression in OFDM systems," *IEEE Commun. Letters*, vol. 10, no. 6, pp. 444–446, Jun. 2006.

[16] I. Cosovic and V. Janardhanam, "Sidelobe suppression in OFDM systems," in *Multi-Carrier Spread-Spectrum*, K. Fazel and S. Kaiser, Eds. Springer, 2006, pp. 473–482.

[17] R. W. Bäuml, R. F. H. Fischer, and J. B. Huber, "Reducing the peak-to-average power ratio of multicarrier modulation by selected mapping," *Electron. Lett.*, vol. 32, no. 22, pp. 2056–2057, Oct. 1996.

[18] C.-D. Chung, "Spectrally precoded OFDM," *IEEE Trans. Commun.*, vol. 54, no. 12, pp. 2173–2185, Dec. 2006.

[19] ——, "Correlatively coded OFDM," *IEEE Trans. Wireless Commun.*, vol. 5, no. 8, pp. 2044–2049, Aug. 2006.

[20] J. van de Beek and F. Berggren, "N-continuous OFDM," *IEEE Commun. Letters*, vol. 13, no. 1, pp. 1–3, Jan. 2009.

[21] J. van de Beek, "Sculpting the multicarrier spectrum: A novel projection precoder," *IEEE Commun. Letters*, vol. 13, no. 12, pp. 881–883, Dec. 2009.

[22] J. Zhang, X. Huang, A. Cantoni, and Y. J. Guo, "Sidelobe suppression with orthogonal projection for multicarrier systems," *IEEE Trans. Commun.*, vol. 60, no. 2, pp. 589–599, Feb. 2012.

[23] G. Dietrich, "A new formulation of the hypermatrix Householder-QR decomposition," *Comput. Methods Appl. Mech. Engrg.*, vol. 9, no. 3, pp. 273–280, Nov. 1976.

[24] R. Schreiber and B. Parlett, "Block reflectors: Theory and computation," *SIAM J. Numer. Anal.*, vol. 25, no. 1, pp. 189–205, Feb. 1988.

[25] *LTE; Evolved Universal Terrestrial Radio Access (E-UTRA); Physical channels and modulation*, European Telecommunications Standards Institute Std., Rev. 3GPP TS 36.211 version 13.0.0 Release 13, Jan. 2016. [Online]. Available: http://www.etsi.org/standards-search

[26] A. S. Householder, "Unitary triangularization of a nonsymmetric matrix," *J. ACM*, vol. 5, no. 4, pp. 339–342, Oct. 1958.

[27] G. H. Golub and C. F. van Loan, *Matrix Computations*, 3rd ed. Johns Hopkins University Press, 1996.

[28] J. Fang, Z. You, I.-T. Lu, J. Li, and R. Yang, "Resource block based precoding schemes for suppressing out-of-band emission," in *Proc. Military Commun. Conf.*, Nov. 2013, pp. 1570–1575.

[29] Y. Zheng, J. Zhong, M. Zhao, and M. Lei, "A low-complexity precoding technique for N-continuous OFDM," in *Proc. Signal Process. Advances Wireless Commun.*, Jun. 2013, pp. 644–648.

[30] C. Bischof and C. van Loan, "The WY representation for products of Householder matrices," *SIAM J. Sci. Stat. Comput.*, vol. 8, no. 1, pp. s2–s13, Jan. 1987.

[31] R. Schreiber and C. van Loan, "A storage-efficient WY representation for products of Householder matrices," *SIAM J. Sci. Stat. Comput.*, vol. 10, no. 1, pp. 53–57, Jan. 1989.

[32] X. Sun and C. Bischof, "A basis-kernel representation of orthogonal matrices," *SIAM J. Matrix Anal. Appl.*, vol. 16, no. 4, pp. 1184–1196, Oct. 1995.